Analytical Methods

Accepted Manuscript

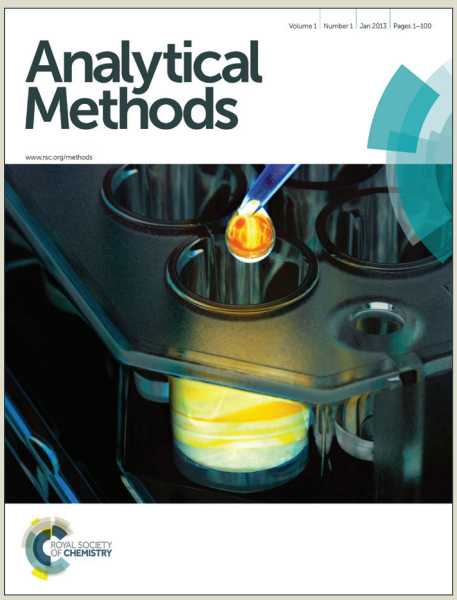

ROYAL SOCIETY OF CHEMISTRY

www.rsc.org/methods

Abstract

In this work, a novel type of core-shell molecularly imprinted magnetic nanoparticles was synthesized and coupled with HPLC for selective extraction and detection of 17β-estradiol (E2) in lake water sample. The synthesis procedure combined surface imprinting technique and facile sol-gel strategy. The morphology, structure, and magnetic property of the obtained products were characterized by transmission electron microscope, X-ray diffraction, Fourier transform infrared spectroscopy, and vibrating sample magnetometer. The adsorption properties of the prepared polymers were investigated by equilibrium rebinding, dynamic adsorption, and selective recognition experiments. The resultant imprinted nanomaterials exhibits not only good dispersibility, stable crystalline, and satisfactory super-paramagnetic property, but also fast kinetics, high capacity (16.87 mg g^{-1}), and favorable selectivity. In addition, the as-synthesized polymers show good reproducibility and could be used at least six cycles of adsorption-desorption without obvious deterioration. The feasibility of the developed method using obtained imprinted polymers as SPE extractant coupled with HPLC for selective isolation and determination of E2 from real water sample was testified. The recovery of E2 in lake water sample was ranged from 94.2 to 98.3% with the relative standard deviation less than 4.3%. The combined method would greatly improve sensitivity and expand practicability of HPLC.

Keywords: Surface imprinting technique, Magnetic separation, Sol-gel strategy, Trace detection

Introduction

The human organism is greatly affected by factors that could mimic or antagonize the normal function of endogenous substance. In typical case, endocrine disrupting compounds (EDCs) are recognized as a group of modalities that interfere with synthesis, secretion, transport, binding, action, and elimination of endocrine hormones in human body.[1,2] Both natural and synthetic estrogens have been found in human living environment, particularly the aquatic matrix which acts as one of inseparable media of man's daily life.[3,4] 17β-estradiol (E2), one of the most active estrogens, can produce various health-related problems even at low concentration, such as early puberty in females, inferior quantity and quality of sperm, altered functions of reproductive organs, obesity and so much as increased rates of some breast, ovarian, testicular, and prostate cancers.[5-9] Therefore, it is of prime importance to develop a simple and reliable analysis method for rapid identification and detection of E2 in complex environmental water matrix.

Currently, for analysis of E2 in intricate medium, immunochemical methods[10,11] such as enzyme-linked immunosorbent assay (ELISA) or radioimmunoassy using specific enzymes are highly selective for aimed compound, but the instability of natural antibodies limits their application to some extent. LC and GC are the most commonly used methods that provide effective detection to analytes, especially using MS or MS/MS as detector.[12,13] However, the first step for analysis is to isolate the component of interest from the complex sample into an injectable solution at detectable concentration. The routine sample pretreatment includes liquid-liquid

extraction (LLE), accelerated solvent extraction (ASE), supercritical fluid extraction (SFE), solid-phase extraction (SPE), etc. Among these, SPE with the merits of simplicity, rapidness, and little depletion of organic solvents has gained much attention. Despite these attractive advantages, the conventional SPE sorbents still need fussy centrifugation and filtration procedures or to be packed into the SPE cartridge, which are time-consuming and complicated. To solve this problem, magnetic SPE technique has been dramatically developed.

Magnetic SPE technique could achieve the magnetic sorbents being easily separated from the solution of analyte in the presence of an external magnetic field. In particular, magnetic Fe_3O_4 nanoparticles (NPs) are the most commonly used sorbent for their good biocompatibility, low toxicity, and easy preparation.[14,15] Gao et al.[16] prepared polypyrrole-coated magnetite nanoparticles with a high π-conjugated structure and hydrophobicity for extraction of estrogens from milk samples. Wei et al.[17] synthesized graphene oxide-modified Fe_3O_4 NPs employed as a sorbent to separate bovine serum albumin in biological sample. Tahmasebi et al.[18] prepared polythiophene-coated Fe_3O_4 super-paramagnetic nanocomposite for extraction and preconcentration of several typical plasticizers from environmental water samples. These magnetic sorbents can achieve rapid phase separation, but the low selectivity might result from the coextraction of interferents from the matrix. Therefore, if magnetic components such as Fe_3O_4 NPs or functionalized Fe_3O_4 NPs could be encapsulated in molecularly imprinted polymers (MIPs), the resultant composite polymers could integrate magnetic property and selectivity for target molecule into

one entity.

Core-shell nano-sized MIPs based on magnetic Fe_3O_4 NPs are usually created through surface imprinting technique, which possess thin imprinted shells with specific recognition sites complementary to the shape, size, and functional groups of predetermined analyte on the surface of magnetic supporters. These MIPs with unique structure own faster mass transfer of molecules into and out of recognition sites and higher adsorption capacity due to high surface-to-volume ratio of materials.[19,20] Meanwhile, owning to the inherent advantages of MIPs such as simple and economical production, reusability, as well as excellent selectivity, such core-shell nano-structured magnetic MIPs have been widely used as novel SPE sorbents with virtues of rapid and selective clean-up and preconcentration before determination.[21,22] HPLC assay is simpler and more widely available in majority of laboratories, but has lower sensitivity compared with GC-MS[23] and LC-MS.[24] Therefore, if HPLC could be combined with magnetic core-shell nanosized MIPs as SPE extractant, it will greatly improve sensitivity and expand practicability of this method for analysis of E2 at low concentration levels in complex environmental water samples.

Herein, a novel type of core-shell imprinted nanoparticles using silica coated Fe_3O_4 NPs as supporters for selective isolation and enrichment of E2 was prepared *via* surface imprinting technique and facile sol-gel polymerization. The obtained imprinted nanomaterials possess thin imprinted shells with tailor-made affinity binding sites and exhibit high binding capacity, fast kinetic, excellent selectivity as

well as satisfactory reusability. The synthetic process is quite simple and different batches of resulting products exhibits good reproducibility as a sorbent for E2. Meanwhile, the obtained polymers coupled with HPLC were successfully applied for determination of trace E2 in environmental aquatic sample.

Experimental

Chemicals

Tetraethoxysilane (TEOS) and 3-aminopropyltriethoxysilane (APTES) were purchased from Alfa Aesar Chemical Company. Ferric chloride hexahydrate ($FeCl_3 \cdot 6H_2O$), anhydrous sodium acetate (NaOAc), ethylene glycol, ethanol, acetonitrile, ammonium hydroxide (25%), and acetic acid were provided by Xi'an Chemicals Ltd. E2, estrone (E1), estriol (E3), and diethylstilbestrol (DES) were obtained from Sigma. All reagents used were of at least analytical grade. The highly purified water (18.0 MΩ cm^{-1}) was obtained from a WaterPro water system (Axlwater Corporation, TY10AXLC1805-2, China) and used throughout the experiments. Environmental water sample was collected from local lake, and stored in precleaned glass bottle.

Apparatus and analytical methods

The instruments used in this study were as follows: Nicolet AVATAR-330 Fourier transform infrared (FT-IR) spectrometer (Thermo Electron Corporation, U.S.A), Tecnai G2 T2 S-TWIN transmission electron microscope (FEI Corporation, Netherlands), LDJ 9600-1 vibrating sample magnetometer (VSM) (LDJ Corporation, U.S.A), and Rigaku D/max/2500v/pc X-ray diffractometer (Rigaku Corporation,

Japan). A Shimadzu HPLC system equipped with LC-10AT pump, SPD-M 10A detector, CTO-10AS column oven, and Shimadzu VP-ODS C18 column (5 μm, 150 mm × 4.6 mm). The column temperature was 30 °C. The mobile phase was acetonitrile-water (65 : 35, v/v) delivered at a flow rate of 1.0 mL min^{-1}, the injection volume was 20 μL, and the column effluent was monitored at 280 nm. Sample solutions were filtered through a nylon 0.22 μm filter before determination.

Preparation of CS-Fe_3O_4@E2-MIPs and CS-Fe_3O_4@NIPs

The monodispersed Fe_3O_4 NPs and the silica-modified Fe_3O_4 NPs (designed as Fe_3O_4@SiO_2) were prepared as our previous work.[25] The core-shell magnetic molecularly imprinted polymers of E2 (designed as CS-Fe_3O_4@E2-MIPs) were prepared through a facile sol-gel process. Briefly, E2 (50 mg) was dissolved in ethanol (20 mL), and mixed with the functional monomer APTES (80 μL). The mixture was stirred for 1 h to form template-monomer complex. Then Fe_3O_4@SiO_2 (0.2 g), TEOS (200 μL), and ammonium hydroxide (600 μL) were added to the above mixture, which began to co-hydrolyse and co-condense after stirring for a few minutes, and allowed to proceed for 3 h at room temperature. The resultant products were rinsed with water until the supernatant was neutral, and ethanol-acetic acid (93:7, 94:6, 95:5, 96:4, and 97:3, v/v) was added as eluent to remove the template molecule E2 at room temperature. The obtained imprinted polymers were collected by an external magnetic field and repeatedly washed with highly purified water, then dried under vacuum. For comparison, non-imprinted magnetic nanoparticles (designed as CS-Fe_3O_4@NIPs) were prepared following the same procedure in the absence of the

template molecule E2.

Binding properties of CS-Fe_3O_4@E2-MIPs and CS-Fe_3O_4@NIPs

In kinetic adsorption test, 20 mg of CS-Fe_3O_4@E2-MIPs or CS-Fe_3O_4@NIPs were suspended in 10 mL of ethanol with E2 at a concentration of 0.15 mg mL^{-1}, and shaken on a reciprocating shaking-table at regular times from 1 min to 15 min. Then the supernatants and polymers were separated by an external magnetic field and the supernatants were filtered through a 0.22 μm nylon filter. The concentration of E2 in the filtrate was measured by HPLC. The adsorption amounts (Q, mg g^{-1}) of CS-Fe_3O_4@E2-MIPs and CS-Fe_3O_4@NIPs to E2 were calculated according to equation (1), and the pseudo-second-order rate kinetic model was applied to fit the kinetic data according to equation (2).

$$Q = \frac{(C_0 - C_e)V}{m} \quad (1)$$

$$\frac{t}{Q_t} = \frac{1}{k_2 Q_e^{\,2}} + \frac{t}{Q_e} = \frac{1}{v_0} + \frac{t}{Q_e} \quad (2)$$

where C_0 and C_e (mg mL^{-1}) are the initial and equilibrium concentration of E2, respectively. V (mL) represents the volume of the E2 solution. m (g) is the mass of the polymers. Q_e and Q_t (mg g^{-1}) are the amount of E2 adsorbed onto CS-Fe_3O_4@E2-MIPs or CS-Fe_3O_4@NIPs at the equilibrium and time t (min), respectively. Value of k_2 (g mg^{-1} min^{-1}) is the rate constant of pseudo-second-order adsorption and v_0 (mg g^{-1} min^{-1}) represents the initial adsorption rate.

In steady-state binding test, 20 mg of CS-Fe_3O_4@E2-MIPs or CS-Fe_3O_4@NIPs were dispersed into 10 mL of ethanol with various E2 concentrations (0.010-0.30 mg mL^{-1}), and incubated for 5 min at room temperature. The separation and detection

procedures were conducted as described in kinetic adsorption test. The saturation binding data were further processed by Langmuir and Freundlich isotherm models according to equation (3) and (4).

$$\frac{C_e}{Q} = \frac{1}{Q_{max} K_L} + \frac{C_e}{Q_{max}} \quad (3)$$

$$\log Q = m \log C_e + \log K_F \quad (4)$$

Where C_e (mg mL^{-1}) is equilibrium concentration of adsorbate, Q (mg g^{-1}) is the amount of E2 bound to CS-Fe_3O_4@E2-MIPs or CS-Fe_3O_4@NIPs at equilibrium, Q_{max} (mg g^{-1}) is the maximum adsorption capacity of the sorbent, K_L (mL mg^{-1}) and K_F (mg g^{-1}) are the Langmuir and Freundlich constant respectively, and m is the Freundlich exponent which represents the heterogeneity of the system.

The selectivity of CS-Fe_3O_4@E2-MIPs was measured using the structural analogues E1, E3, and DES. 10 mL of the mixed standard solution of E1, E2, E3, and DES at initial concentration of 0.15 mg mL^{-1} was incubated with 20 mg of CS-Fe_3O_4@E2-MIPs and CS-Fe_3O_4@NIPs for 5 min, and then the operating sequence was the same as kinetic adsorption test. The specific recognition property of CS-Fe_3O_4@E2-MIPs was evaluated by imprinting factor (*IF*), which was calculated according to equation (5), and the selectivity factor (*SC*) defined as expressed in equation (6).

$$IF = \frac{Q_{MIP}}{Q_{NIP}} \quad (5)$$

$$SC = \frac{IF_t}{IF_c} \quad (6)$$

Where Q_{MIP} and Q_{NIP} (mg g^{-1}) represent the adsorption capacity of E2 on

CS-Fe_3O_4@E2-MIPs and CS-Fe_3O_4@NIPs, respectively. IF_t and IF_c are the imprinting factors for template molecule and competitive molecule.

Reproducibility and reusability of CS-Fe_3O_4@E2-MIPs and CS-Fe_3O_4@NIPs

To investigate the reproducibility of resultant polymers, 20 mg of six batches of CS-Fe_3O_4@E2-MIPs and CS-Fe_3O_4@NIPs prepared on different days were added to 10 mL of E2 solution at a concentration of 0.15 mg mL^{-1}. After incubation for 5 min at room temperature, the supernatants and polymers were separated by an external magnetic field and the supernatants were filtered through a 0.22 μm nylon filter. Then the concentration of E2 in the filtrate was measured by HPLC.

To estimate the reusability of CS-Fe_3O_4@E2-MIPs and CS-Fe_3O_4@NIPs, adsorption-desorption procedure was repeated for 6 times for E2 by using the same polymers. Typically, 20 mg of polymers were added to 10 mL of E2 solution at a concentration of 0.15 mg mL^{-1} and incubated at room temperature, while gently shaken on a reciprocating shaking-table for 5 min. Then, CS-Fe_3O_4@E2-MIPs and CS-Fe_3O_4@NIPs were removed by a magnet and the bound amount of E2 was quantified by HPLC. The reused polymers were eluted with ethanol-acetic acid (95:5, v/v) for 6 h to ensure complete removal of the residual E2 in the polymers and washed with highly purified water for several times, then dried under vacuum and explored in succeeding adsorption-regeneration cycles.

Determination of E2 in lake water sample

The lake water sample collected from the Xing Qing Park (Xi'an, China) was spiked with E2 at three levels (1.0, 10.0, and 100.0 ng mL^{-1}) for analysis. 100 mg of

CS-Fe_3O_4@E2-MIPs or CS-Fe_3O_4@NIPs were added to 100 mL of the lake water sample containing E2, respectively. After 5 minutes of incubation on an oscillator, the CS-Fe_3O_4@E2-MIPs or CS-Fe_3O_4@NIPs were isolated by an external magnet. The CS-Fe_3O_4@E2-MIPs or CS-Fe_3O_4@NIPs which absorbed target molecules were eluted with a mixture of ethanol-acetic acid (95:5, v/v) solution, and then the elution was collected and evaporated to dry under a stream of nitrogen. Finally, the residue of the elution was dissolved in 0.5 mL of acetonitrile and measured by HPLC-UV.

Results and discussion

Preparation of imprinted nanomaterials

The synthesis of CS-Fe_3O_4@E2-MIPs is illustrated in Fig. 1. First, Fe_3O_4 NPs were prepared through a modified solvothermal reaction, and then encapsulated by silica shells through a mild sol-gel process. The silica coating could not only insulate the magnetic dipolar attraction between magnetic NPs, but also supply a silica-like surface for easy modification with various groups.[26] Next, the template-monomer complex was obtained adopting E2 as template and APTES as functional monomer through the hydrogen bonding interactions between the amino groups of APTES and hydroxyl groups of E2. Then, using TEOS as a cross-linking agent, a polymeric network molded around the template E2 was obtained by the reaction between the Fe_3O_4@SiO_2 and template-monomer complex. Finally, CS-Fe_3O_4@E2-MIPs with imprinted cavities complementary to the template E2 in shape, size, and orientation of functional groups were obtained after the removal of the embedded templates.

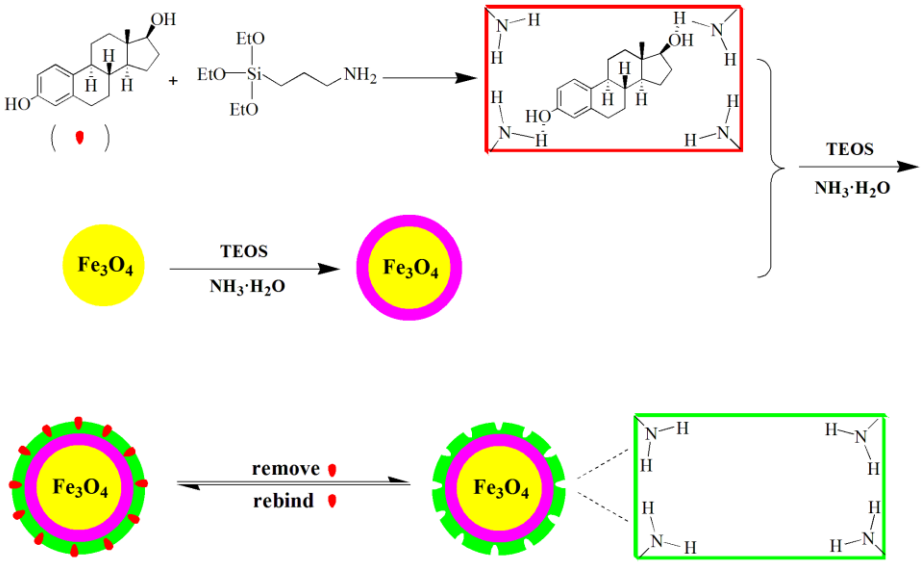

Fig. 1. Scheme of the synthetic route for CS-Fe_3O_4@E2-MIPs.

The elution step is a crucial procedure to ensure that the template molecules are completely removed, which could avoid the interference of quantification caused by template leaking. Thus, the volume ratio of ethanol to HAc was investigated. The results were shown in Fig. S1. It is obvious that the ratio of ethanol to HAc has distinct effect on the recovery of E2 absorbed by CS-Fe_3O_4@E2-MIPs. With increasing the volume of HAc, the recovery of E2 by CS-Fe_3O_4@E2-MIPs exhibits an upward trend and attains a pinnacle at the volume ratio of 95:5. Therefore, the volume ratio of ethanol to HAc (v/v, 95:5) was chosen as the optimum eluting solvent.

The adsorption capacity and imprinting effect of CS-Fe_3O_4@E2-MIPs towards template molecule are greatly influenced by functional monomer, which could discern the template through the interactions between template molecules and the functional groups with predetermined orientation in the polymer network. Therefore, the volume fraction of functional monomer in ethanol solution was investigated ranging from 0.1% to 0.6% for obtaining the optimal polymerization condition. The results of the

adsorption capacity (*Q*) and imprinting factor (*IF*) are shown in Fig. 2. With increasing the volume fraction of functional monomer, all the imprinted polymers adsorb larger amount of template molecule than the non-imprinted polymers, indicating the formation of recognition sites in the imprinted polymers. Furthermore, we could observe that the *Q* and *IF* exhibit an upward trend with increasing the volume fraction of functional monomer from 0.1% to 0.3% and attain a pinnacle at the volume fraction of 0.4%, manifesting that the augment in the number of recognition cavities through the adequate interactions between enough amount of functional monomer and template. A followed drop is observed with further increasing the volume fraction from 0.4% to 0.6%. The reason may be that excessive functional monomers promote self-aggregation, or the shells of imprinted polymers become thicker, leading to difficult removal of template, which both result in a drop in the number of recognition sites. Therefore, the volume fraction of functional monomer of 0.4% was adopted for preparation of CS-Fe_3O_4@E2-MIPs.

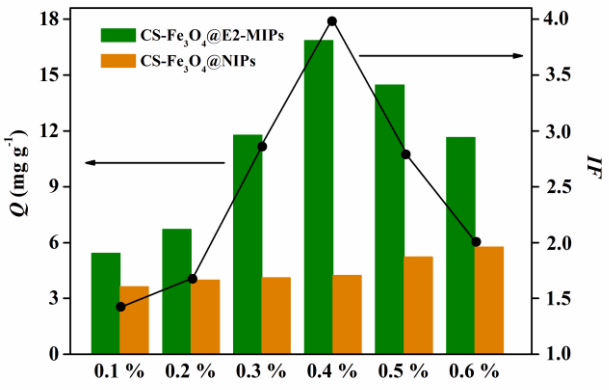

Fig. 2. Effect of the volume fractions of functional monomer on the imprinting performance of CS-Fe_3O_4@E2-MIPs and CS-Fe_3O_4@NIPs.

Characterization of prepared magnetic nanomaterials

Representative TEM images of Fe_3O_4, Fe_3O_4@SiO_2, and CS-Fe_3O_4@E2-MIPs are shown in Fig. 3. It can be obviously seen that Fe_3O_4, Fe_3O_4@SiO_2, and CS-Fe_3O_4@E2-MIPs all exhibit spherical morphology and homogeneous distribution. The pure Fe_3O_4 NPs were obtained in uniform spherical shape with a diameter of about 200 nm (Fig. 3A). After coating with thin silica shells, the size of resultant Fe_3O_4@SiO_2 increased to around 220 nm (Fig. 3B), corresponding to a 10 nm thick SiO_2 layer deposited on the surface of Fe_3O_4 NPs. The TEM image in Fig. 3C displays the morphological structure of CS-Fe_3O_4@E2-MIPs after the template-monomer complex was anchored on the surface of Fe_3O_4@SiO_2, while the polymer shell could not be clearly distinguished with SiO_2 layers probably due to the close contrast of the imprinted polymer shell and the silica shell. However, the presence of the polymer shell could still be evidenced by significantly increased shell thickness of CS-Fe_3O_4@E2-MIPs to about 15 nm in comparison with silicon layer, indicating that the thickness of the imprinted layer was approximately 5 nm, which would be beneficial for the mass transfer between solution and the surface of CS-Fe_3O_4@E2-MIPs.

To ascertain the successful synthetic process of CS-Fe_3O_4@E2-MIPs, each preparation stage was tracked by FT-IR spectra. The characteristic peaks of the stretch of Fe-O group for Fe_3O_4, Fe_3O_4@SiO_2, and CS-Fe_3O_4@E2-MIPs are all observed around 586 cm^{-1} (Fig. 4A). The adsorption peaks at 3442 cm^{-1} and 1638 cm^{-1} are assigned to stretching and bending vibrations of O-H (Fig. 4A-a), suggesting that the surface of Fe_3O_4 has hydroxyl groups.[27] Compared with the infrared characteristic

peaks of pure Fe_3O_4, the strong peak at approximately 1100 cm^{-1} is attributed to the stretching vibration of Si-O-Si (Fig. 4A-b), indicating that the silica layer was coated on the surface of Fe_3O_4 NPs. The typical peak at 3442 cm^{-1} arising from N-H stretching vibration might overlap with that of O-H stretching vibration,[28] but the relatively high intensity of the peak and bending vibration of N-H at 1550 cm^{-1} still reveal the contribution of $-NH_2$ groups (Fig. 4A-c). The existence of these typical peaks proved that the template-monomer complex layer was deposited onto the surface of Fe_3O_4@SiO_2.

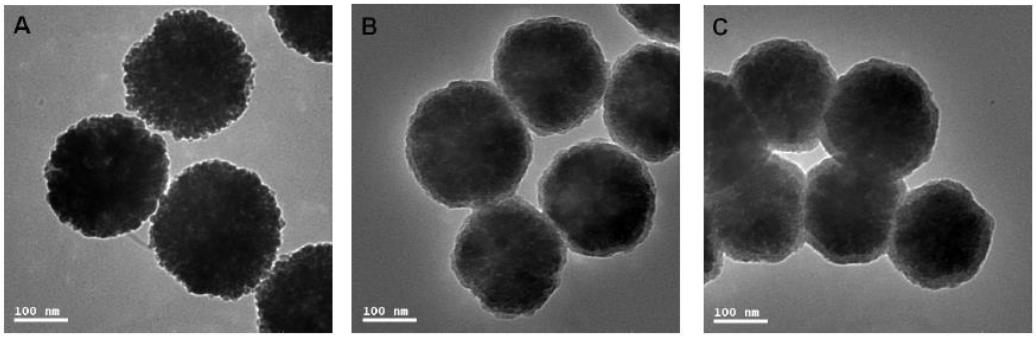

Fig. 3. TEM images of Fe_3O_4 (A), Fe_3O_4@SiO_2 (B), and CS-Fe_3O_4@E2-MIPs (C).

The XRD patterns of the synthesized Fe_3O_4, Fe_3O_4@SiO_2, and CS-Fe_3O_4@E2-MIPs are illustrated in Fig. 4B. In the 2θ region of 20-80°, six relatively discernible strong diffraction peaks corresponded to Fe_3O_4 (2θ = 30.2°, 35.6°, 43.2°, 53.5°, 57.2°, and 62.8°) are observed in the curves of three samples, and the peak positions at the corresponding 2θ values are indexed as (220), (311), (400), (422), (511), and (440), respectively, which match well with the database of magnetite in the JCPDS-International Center for Diffraction Data (JCPDS Card: 19-629) file. The results confirm that the crystalline of the resultant polymers remained unchanged during the process of synthesis, and both Fe_3O_4@SiO_2 and CS-Fe_3O_4@E2-MIPs are

composed of pure Fe_3O_4 with a cubic inverse spinel structure.[29]

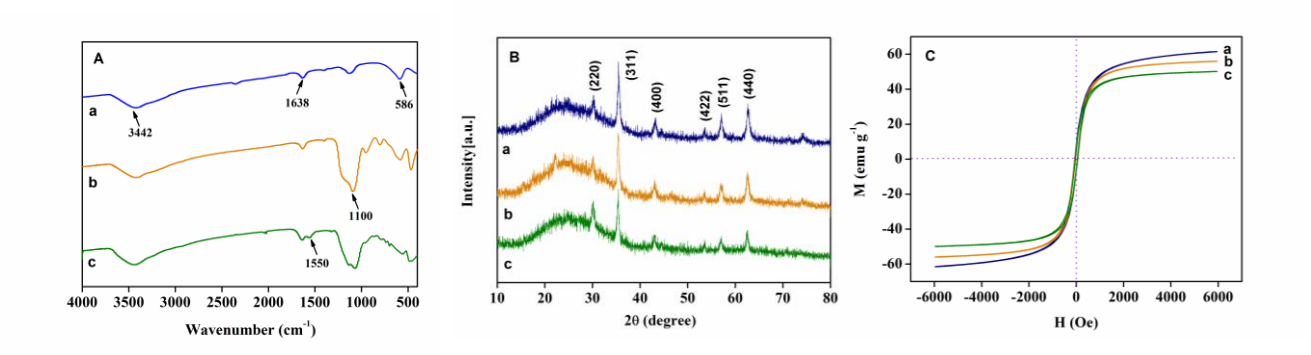

Fig. 4. FT-IR spectra (A), XRD patterns (B), and magnetization curves (C) of Fe_3O_4 (a), Fe_3O_4@SiO_2 (b), and CS-Fe_3O_4@E2-MIPs (c).

In general, the magnetic material should possess sufficient magnetic property for potential magnetic separation in practical application. Therefore, the VSM analysis was employed to investigate the magnetic properties of Fe_3O_4, Fe_3O_4@SiO_2, and CS-Fe_3O_4@E2-MIPs. As shown in Fig. 4C, the three magnetic hysteresis loops with similar shape of S-like curves are all symmetrical to the origin and there is no hysteresis, both remanence and coercivity are approximately zero, confirming that samples are super-paramagnetic. The saturation magnetization values of Fe_3O_4@SiO_2 and CS-Fe_3O_4@E2-MIPs are 55.99 and 50.15 emu g^{-1}, which reduce about 5 and 10 emu g^{-1} respectively in comparison with that of pure Fe_3O_4 (61.51 emu g^{-1}). The decreases are expected because the silica and imprinted coatings could shield the magnetite, while the relatively small decrease of magnetization value from pure Fe_3O_4 NPs to CS-Fe_3O_4@E2-MIPs demonstrates that the imprinted layer is quite thin, which might be effective to absorb and desorb template molecules between solution and CS-Fe_3O_4@E2-MIPs. Meanwhile, the saturation magnetization value of

CS-Fe_3O_4@E2-MIPs is higher than those of other literatures reported for imprinted non-thin films,[30,31] making them to be separated easily and rapidly from the suspension under an external magnetic field.

Adsorption kinetics

The adsorption kinetics was carried out using an initial concentration of E2 at 0.15 mg mL^{-1} for CS-Fe_3O_4@E2-MIPs and CS-Fe_3O_4@NIPs to determine the rate of the adsorption process. The results are presented in Fig. 5A, which reveal a rapid increase of the binding capacity in the first 4 min due to a large amount of empty recognition cavities on the surface of the polymers that can bind E2 easily with less resistance. Then, since most of the binding sites have been occupied, the adsorption rate exhibits a slower increase to reach the adsorption equilibrium after 5 min. In this work, the adsorption takes about 5 min to approach the equilibrium which is much shorter than those of most published reports for E2-imprinted polymers.[32,33] Thus, it is believed that the formed thin imprinted shell with much recognition sites situated on could dramatically improve the mass transfer for easy diffusion of E2 into the imprinted cavities.

In order to further investigate the adsorption kinetic mechanism, the kinetic data obtained was analyzed using pseudo-second-order rate equation. As shown in Table 1, pseudo-second-order model fits the experimental data quite well with relatively high correlation coefficients ($r > 0.99$). The initial sorption rate v_0 of imprinted polymers (10.59 mg g^{-1} min^{-1}) is quite high, indicating that the adsorption of E2 onto CS-Fe_3O_4@E2-MIPs is a fast process that attributes to a high density of active

recognition sites on the surface of the polymers. Moreover, it is possible to conclude that the chemical course could be the rate-limiting step in the adsorption process.[34]

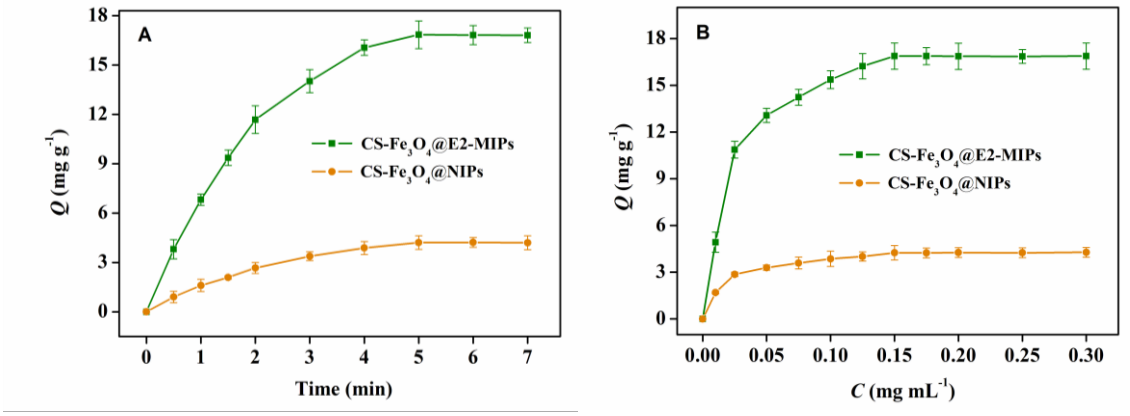

Fig. 5. Adsorption kinetics (A) and isotherms (B) of CS-Fe_3O_4@E2-MIPs and CS-Fe_3O_4@NIPs towards E2.

Adsorption isotherms

To investigate the affinity of CS-Fe_3O_4@E2-MIPs and CS-Fe_3O_4@NIPs, a steady-state binding test was carried out towards a series of solutions with different concentrations of E2 and the results are depicted in Fig. 5B. It could be seen that the adsorption capacity of CS-Fe_3O_4@E2-MIPs increases rapidly along with the increasing of the concentration of E2 from 0.010 to 0.15 mg mL^{-1} and comes to a saturation platform over 0.15 mg mL^{-1}. It is not difficult to observe that the amount of E2 bound to CS-Fe_3O_4@E2-MIPs is much higher than that of CS-Fe_3O_4@NIPs, suggesting that the recognition sites on the surface of imprinted polymers possess "memory effect" for template molecules on spatial position and chemical effect.

Table 1 Equations and parameters of adsorption kinetics and isotherms of CS-Fe_3O_4@E2-MIPs and CS-Fe_3O_4@NIPs.

Model	Equations and Parameters	CS-Fe_3O_4@E2-MIPs	CS-Fe_3O_4@NIPs
Pseudo-second-order rate kinetic	Equation	$t/Q_t = 0.09444 + 0.04309\ t$	$t/Q_t = 0.4383 + 0.1631\ t$
	Q_e (mg g^{-1})	23.21	6.131
	k_2 (g mg^{-1} min^{-1})	0.01966	0.06069
	v_0 (mg g^{-1} min^{-1})	10.59	2.282
	r	0.9912	0.9912
Langmuir isotherm	Equation	$C_e/Q = 2.762 \times 10^{-4} + 0.05810\ C_e$	$C_e/Q = 3.140 \times 10^{-3} + 0.2192\ C_e$
	Q_{max} (mg g^{-1})	17.21	4.562
	K_L (mL mg^{-1})	210.4	69.81
	r	0.9994	0.9995
Freundlich isotherm	Equation	$\log Q = 1.3634 + 0.1620\ \log C_e$	$\log Q = 0.8081 + 0.2345\ \log C_e$
	K_F (mg g^{-1})	23.09	6.428
	m	0.1620	0.2345
	r	0.9754	0.9572

To further investigate the adsorption behavior of CS-Fe_3O_4@E2-MIPs and CS-Fe_3O_4@NIPs, the Langmuir and Freundlich isotherm models were applied to fit the equilibrium data and the results are presented in Table 1. Langmuir isotherm model is basically used for monolayer adsorption onto a surface with a homogeneous system, while Freundlich isotherm model is suitable for multilayer adsorption of heterogeneous system which is not restricted to the formation of the monolayer. The Langmuir isotherm model ($r > 0.99$) is better fit the adsorption of E2 onto CS-Fe_3O_4@E2-MIPs than Freundlich isotherm model ($r < 0.98$). Furthermore, the maximum amount of adsorption calculated from the intercept of Langmuir linear equation (17.21 mg g^{-1} for MIPs and 4.562 mg g^{-1} for NIPs) is close to that of experimental results (16.87 mg g^{-1} for MIPs and 4.251 mg g^{-1} for NIPs). It could

conclude that the adsorption of E2 onto CS-Fe_3O_4@E2-MIPs and CS-Fe_3O_4@NIPs may conform to monolayer adsorption.[35,36]

Specific recognition of CS-Fe_3O_4@E2-MIPs

The binding specific experiments of CS-Fe_3O_4@E2-MIPs and CS-Fe_3O_4@NIPs were carried out selecting three other estrogens (E1, E3, and DES) as the analogues whose molecular structures are displayed in Fig. S2. As shown in Table 2, the *Q* and *IF* of CS-Fe_3O_4@E2-MIPs for E2 are 12.07 mg g^{-1} and 5.77, which are higher than those of three other estrogens, suggesting that imprinted polymers have relatively high affinity for E2 than its analogues. Meanwhile, the high *SC* that greater than 1.7 further strengthens the conclusion. Moreover, the recognition capacity of CS-Fe_3O_4@E2-MIPs for three analogues have appreciable difference with the order of E1＞E3＞DES. This may be due to the different molecular structures, E3 and E1 possess the similar skeleton with E2, except that E3 has an exceeded hydroxyl group in position 16, and E1 has a carbonyl group in position 17 substituted for the hydroxyl group of E2, implying the weaker ability to form hydrogen bonds compared with hydroxyl group. Although E3 has one more hydroxyl group compared with E2, meaning more opportunities to form hydrogen bonds with functional monomer APTES, the -OH in position 16 could also interfere the -OH in position 17 that suspects to preferentially bind to the functional monomer in the specific cavities through steric hindrance effect.[37] While DES has two phenol hydroxyl groups, holding different carbon skeleton from E2, which is the main factor for the low capacity, because the size and shape of imprinted cavities are not suitable for DES.

These results demonstrate that the imprinted cavities play an important role in the process of specific recognition and the resulting imprinted polymers in this work exhibit satisfactory imprinting effect.

Table 2

The adsorption capacities, imprinting factors, and selectivity coefficients of E2, E1, E3, and DES for CS-Fe_3O_4@E2-MIPs and CS-Fe_3O_4@NIPs.[a]

Analytes	Q_{MIP}（mg g^{-1}）	Q_{NIP}（mg g^{-1}）	*IF*	*SC*
E2	12.07	2.092	5.77	—
E3	4.781	1.681	2.84	2.03
E1	5.536	1.647	3.36	1.72
DES	1.542	1.226	1.26	4.58

[a] In this experiment, 20 mg of CS-Fe_3O_4@E2-MIPs and CS-Fe_3O_4@NIPs were incubated with the mixture of E2, E1, E3, and DES at a concentration of 0.15 mg mL^{-1} in 10 mL of ethanol for 5 min at room temperature.

Reproducibility and reusability of CS-Fe_3O_4@E2-MIPs and CS-Fe_3O_4@NIPs

The reproducibility of the obtained imprinted magnetic nanomaterials was investigated by using six batches of CS-Fe_3O_4@E2-MIPs and CS-Fe_3O_4@NIPs prepared on different days, and the measurements all replicated five times in parallel. The average adsorption capacity of each batch and the relative standard deviation (RSD) are listed in Table S1. The results show that the reproducibility of six batches of CS-Fe_3O_4@E2-MIPs and CS-Fe_3O_4@NIPs are all satisfactory with a RSD less than 9.4%.

The reusability of adsorbents is considered to have a great cost benefit for the polymers in practical applications. Therefore, six consecutive adsorption-desorption cycles were carried out by using the same CS-Fe_3O_4@E2-MIPs to investigate their stability. The results shown in Fig. S3 manifest that the imprinted polymers are relatively stable whose adsorption capacity still holds at almost a steady value of

96.8% after six regeneration cycles, indicating that recognition, interaction, and adsorption processes are occurred reversibly and the method applied for elution is suitable for purification procedure. The slightly decrease of adsorption capacity might ascribe to the fact that some recognition sites in the network of CS-Fe_3O_4@E2-MIPs could be masked after regeneration or destructed after rewashing. On the other hand, the affinity of CS-Fe_3O_4@NIPs is nonspecific and the effect of washing is negligible. The results further testify that the polymers obtained are a promising candidate for applying in large scale and economizing the expenditure.

Evaluation of the method

Generally, a pretreatment process is required before instrument analysis, while the conventional treatment (such as C_{18}-SPE, see Fig. S4) could not provide sufficient extraction to meet the detection of trace contaminants due to poor selectivity. Therefore, CS-Fe_3O_4@E2-MIPs were used as solid phase extractant coupled with HPLC-UV for selective enrichment and determination of E2. The analytical performance of the method was validated, including linear range, limit of detection (LOD), limit of quantification (LOQ), accuracy, and reproducibility. Good linearity (r = 0.9996) was obtained in the range of 1.0-200.0 ng mL^{-1}. LOD, indicating the sensitivity of the analytical method, was evaluated and found to be 0.10 ng mL^{-1} (S/N = 3). LOQ (S/N=10) was 0.38 ng mL^{-1}. To evaluate the accuracy of the developed method, the samples spiked with three levels (1.0, 10.0, and 100.0 ng mL^{-1}) of E2 were analyzed and each concentration was measured five times. The recovery of E2 was ranged from 94.2 to 98.3% with RSD less than 4.3% (Table S2). These results

demonstrate that CS-Fe_3O_4@E2-MIPs coupled with HPLC could satisfy the need of selective isolation and determination of trace E2 in water sample. The reproducibility of the method was determined by the intra-day and inter-day precision at three different concentrations of 1.0, 10.0, and 100.0 ng mL^{-1}, respectively. The results showed that the RSD of intra-day precision was 3.2-4.3%, while that of inter-day precision was 3.9-5.8%, indicating good reproducibility of the method. Different methods for determination of E2 are summarized briefly in Table 3. As can be seen, the present approach have lower LODs than those of other reported methods followed by HPLC-UV analysis,[38,39] and comparable LODs in comparison with the method of UPLC-MS-MS[24] and GC-MS.[23] Through the comparison, we could conclude that the method developed in this work is simple, time-saving, reliable, effective, and sensitive.

Table 3

Comparison of LODs with other published methods for the determination of E2.

Analytes	Extraction method	Analytical system	LODs	Reference
E2	MISPE[a]	HPLC-UV	7.00 ng g^{-1}	[38]
E2	HF-LLLME[b]	HPLC-UV	0.66 ng mL^{-1}	[39]
E2	ZIF-8-MSPE[c]	UPLC-MS-MS	0.05 ng mL^{-1}	[24]
E2	—	GC-MS	3.8 ng L^{-1}	[23]
E2	CS-Fe_3O_4@E2-MIPs	HPLC-UV	0.10 ng mL^{-1}	this work

[a] MISPE：Molecularly imprinted solid phase extraction.

[b] HF-LLLME：Hollow fiber liquid-liquid-liquid microextraction.

[c] ZIF-8-MSPE：Zeolitic imidazolate framework-8 micro-solid-phase extraction.

Real sample analysis

The validated method was applied for selective enrichment and determination of E2 in lake water sample. The chromatograms of lake water sample spiked with E2 at the concentration of 100.0 ng mL^{-1}, and the extraction of adsorbed CS-Fe_3O_4@E2-MIPs

are exhibited in Fig. S4. The peak of E2 could not be observed from chromatogram of the spiked lake water sample (Fig. S5A). After the enrichment of spiked lake water sample with CS-Fe_3O_4@E2-MIPs, and washing by ethanol-acetic acid (95:5, v/v), the peak of E2 emerges distinctly at 12.21 min in accordance with E2 standard peak time (Fig. S5C) and the other interference peaks are almost eliminated (Fig. S5B). The results confirm that E2 in spiked lake water sample is selectively isolated by CS-Fe_3O_4@E2-MIPs and could be enriched by the washing step. The sample preparation method using CS-Fe_3O_4@E2-MIPs as solid phase extractant in this work not only save time, human labor, and chemical reagents, but also exhibit satisfactory selectivity and anti-interference ability.

Conclusion

A low-cost and simple method was developed to prepare core-shell structured molecularly imprinted nanocomposites using facile sol-gel polymerization reaction based on Fe_3O_4 NPs coated with silica. The synthetic polymers combined the merits of surface molecular imprinting and magnetic separation. The imprinted nanomaterials possess fast kinetics, high binding capacity, and satisfactory selectivity towards aimed molecules and have favorable reusability with almost no deterioration after six repeated cycles. Different batches of imprinted polymers show good reproducibility. The prepared imprinted nanomaterials integrated HPLC were successfully applied in the isolation and determination of E2 from lake water sample, demonstrating potential value in separation and detection of environmental pollutant so as to provide a feasible and alternative solution for monitoring the safety of environmental water.

Acknowledgements

The authors are grateful for financial support from the National Natural Science Foundation of China (No. 21305107) and the Fundamental Research Funds for the Central Universities (Nos. 08143081, 08142034).

Reference

1. J. B. Gadd, L. A. Tremblay and G. L. Northcott, *Environ. Pollut.*, 2010, **158**, 730-736.
2. D. Fatta-Kassinos, I. K. Kalavrouziotis, P. H. Koukoulakis and M. I. Vasquez, *Sci. Total Environ.*, 2011, **409**, 3555-3563.
3. M. Grassi, L. Rizzo and A. Farina, *Environ. Sci. Pollut. Res.*, 2013, **20**, 3616-3628.
4. M. S. Souza, P. Hallgren, E. Balseiro and L. A. Hansson, *Environ. Pollut.*, 2013, **178**, 237-243.
5. V. Okoh, A. Deoraj and D. Roy, *Biochim. Biophys. Acta*, 2011, **1815**, 115-133.
6. W. Y. Hu, G. B. Shi, D. P. Hu, J. L. Nelles and G. S. Prins, *Mol. Cell. Endocrinol.*, 2012, **354**, 63-73.
7. A. Tabata, S. Kashiwada, Y. Ohnishi, H. Ishikawa, N. Miyamoto, M. Itoh, Y. Magara, *Water Sci.Technol.*, 2001, **43**, 109-116.
8. A. Alum, Y. Yoon, P. Westerhoff, M. Abbaszadegan, *Environ. Toxicol.*, 2004, **19**, 257-264.
9. J. Y. Hu, S. J. Cheng, T. Aizawa, Y. Terao, S. Kunikane, *Environ. Sci. Technol.*, 2003, **37**, 5665-5670.
10. S. K. Garnayak, J. Mohanty, T. V. Rao, S. K. Sahoo and P. K. Sahoo, *Aquaculture*, 2013, **392-395**, 148-155.
11. A. Feswick, G. T. Ankley, N. Denslow, L. E. Ellestad, M. Fuzzen, K. M. Jensen, K. Kroll, A.

Lister, D. L. MacLatchy, M. E. McMaster, E. F. Orlando, M. R. Servos, G. R. Tetreault, M. R. Van Den Heuvel and K. R. Munkittrick, *Environ. Toxicol. Chem.*, 2014, **33**, 847-857.

12. C. M. Lu, M. T. Wang, J. Mu, D. C. Han, Y. P. Bai and H. Q. Zhang, *Food Chem.*, 2013, **141**, 1796-1806.
13. C. Ripollés, M. Ibáñez, J. V. Sancho, F. J. López and F. Hernández, *Anal. Methods*, 2014, **6**, 5028-5037.
14. W. B. Zhang, C. X. Sun and X. A. Yang, *Anal. Methods*, 2014, **6**, 2876-2882.
15. M. M. Tian, D. X. Chen, Y. L. Sun, Y. W. Yang and Q. Jia, *RSC Adv.*, 2013, **3**, 22111-22119.
16. Q. Gao, D. Luo, M. Bai, Z. W. Chen and Y. Q. Feng, *J. Agric. Food Chem.*, 2011, **59**, 8543-8549.
17. H. Wei, W. S. Yang, Q. Xi and X. Chen, *Mater. Lett.*, 2012, **82**, 224-226.
18. E. Tahmasebi, Y. Yamini, M. Moradi and A. Esrafili, *Anal. Chim. Acta*, 2013, **770**, 68-74.
19. S. Han, X. Li, Y. Wang and C. Su, *Anal. Methods*, 2014, **6**, 2855-2861.
20. Y. Li, C. K. Dong, J. Chu, J. Y. Qi and X. Li, *Nanoscale*, 2011, **3**, 280-287.
21. Z. K. Lin, W. J. Cheng, Y. Y. Li, Z. R. Liu, X. P. Chen and C. J. Huang, *Anal. Chim. Acta*, 2012, **720**, 71-76.
22. G. Giakisikli and A. N. Anthemidis, *Anal. Chim. Acta*, 2013, **789**, 1-16.
23. N. Migowska, M. Caban, P. Stepnowski and J. Kumirska, *Sci. Total Environ.*, 2012, **441**, 77-88.
24. Y. H. Wang, S. G. Jin, Q. Y. Wang, G. H. Lu, J. J. Jiang and D. R. Zhu, *J. Chromatogr. A*, 2013, **1291**, 27-32.
25. R. X. Gao, X. R. Mu, J. J. Zhang and Y. H. Tang, *J. Mater. Chem. B*, 2014, **2**, 783-792.

26. D. K. Yi, S. S. Lee and J. Y. Ying, *Chem. Mater.*, 2006, **18**, 2459-2461.

27. S. Mohapatra, N. Pramanik, S. Mukherjee, S. K. Ghosh and P. Pramanik, *J. Mater. Sci.*, 2007, **42**, 7566-7574.

28. Q. W. Peng, J. Gan, S. F. Wang, L. B. Kong, G. R. Chen, Y. X. Yang and G. J. Huang, *Ind. Eng. Chem. Res.*, 2013, **52**, 7713-7717.

29. F. X. Chen, S. L. Xie, J. H. Zhang and R. Liu, *Mater. Lett.*, 2013, **112**, 177-179.

30. L. G. Chen and B. Li, *Food Chem.*, 2013, **141**, 23-28.

31. M. Zhang, Y. Z. Wang, X. P. Jia, M. Z. He, M. L. Xu, S. Yang and C. J. Zhang, *Talanta*, 2014, **120**, 376-385.

32. S. Wang, Y. Li, M. J. Ding, X. L. Wu, J. H. Xu, R. Y. Wang, T. T. Wen, W. Y. Huang, P. Zhou, K. F. Ma, X. M. Zhou, S. H. Du, *J. Chromatogr. B*, 2011, **879**, 2595-2600.

33. S. Wang, R. Y. Wang, X. L. Wu, Y. Wang, C. Xue, J. H. Wu, J. L. Hong, J. Liu, X. M. Zhou, *J. Chromatogr. B*, 2012, **905**, 105-112.

34. C. H. Hu, J. Deng, Y. B. Zhao, L. S. Xia, K. H. Huang, S. Q. Ju and N. Xiao, *Food Chem.*, 2014, **158**, 366-373.

35. F. F. Chen, X. Y. Xie and Y. P. Shi, *J. Chromatogra. A*, 2013, **1300**, 112-118.

36. I. Koç, G. Baydemir, E. Bayram, H. Yavuz and A. Denizli, *J. Hazard. Mater.*, 2011, **192**, 1819-1826.

37. T. H. Jiang, L. X. Zhao, B. L. Chu, Q. Z. Feng, W. Yan and J. M. Lin, *Talanta*, 2009, **78**, 442-447.

38. C. D. Zhao, X. M. Guan, X. Y. Liu and H. X. Zhang, *J. Chromatogr. A*, 2012, **1229**, 72-78.

39. B. B Chen. Y. L. Huang, M. He and B. Hu, *J. Chromatogr. A*, 2013, **1305**, 17-26.